Dear editor,

Here we submit a revised manuscript by *Li* et al., entitled "Mixing state and sources of submicron regional background aerosols in the North Qinghai-Tibetan Plateau and the influence of biomass burning". The point-point responses were listed as below.

We carefully revised the manuscript based on the reviewers' comments. Correspondence and phone calls about the paper should be directed to *Weijun Li* at the following address, phone, and e-mail address:

Weijun Li, Ph.D. Prof.
Environment Research Institute
Shandong University
Shanda Nanlu 27, Jinan, Shandong 250100, China
Phone: +086-531-88364675
Email: liweijun@sdu.edu.cn

Best regards,
Sincerely yours,
Weijun Li on behalf of the coauthors

MS NO.: acp-2015-437

Thanks for The referee#1's comments. Those comments are all valuable and helpful for improving our paper. We answered the comments carefully and have made corrections in the submitted manuscript. The corrections and the responses are as following:

1. Page 24372, line 10-11, here author said "however, aerosols of the vast grasslands of the northern TP have not been studied".

a) It is better to briefly state why it is necessary to characterize the aerosols from the grassland atmosphere, if the physicochemical properties of the grassland aerosols are different from those in other places of TP?

b) Page 24372, line 18-20, what is the definition of age? Why aged aerosols represent the typical chemical composition of this continental background region? If this means that fresh aerosols are very less at the sampling site and most of airborne particles are long-range transported?

Response 1 a): We added the reasons why we do study aerosol particles in grassland over the TP.

"Grassland is one of the largest geomorphology in the TP. There are only a few herdsmen and farmers living in the vast grasslands of the norther TP. Air pollutants from anthropogenic and natural sources can be easily transported over low bushes in the grasslands under high wind speed in north TP (Figure S1). However, aerosols in the troposphere have not been studied over the vast grassland in the northern TP."

Response 1 b): Here we deleted the sentence based on the logic in the paragraph. We added the definition about the "aged" particles in section 4.3

2. Page 24373, section 2.1,

a) what is the altitude of the sampling site? This information is important.

b) The density of particles is assumed to be 2 g/cm3, what is the rationale?

Response 2 a): We added

Response 2 b): We usually used the value to calculate the size cut off of the impactor. We consider ammonium sulfate (1.77 g/cm^3), mineral dust (2.6 g/cm^3), and organic matter (1.5 g/cm^3) as the major aerosol types. The average density (calculated at 1.96) of the mixed aerosol particles was assumed to 2 g/cm3.

3. Page 24376 and 24391, Table 1, it's better to give more data such as the standard

deviation, minimum, and maximum values, because data here are statistic numbers; the mean value itself does not give enough information.

Response 3: Thank you. We add standard deviation, min, and max value.

Table 1 Concentrations of six air pollutants during the sampling period, two pollution periods, and clean period

Pollutants	All data		polluted period-1		polluted period-2		other period	
	mean ±SD Max, Min	n	mean ±SD Max, Min	n	mean ±SD Max, Min	n	mean ±SD Max, Min	n
$PM_{2.5}$	17.06 ±11.39 68.70, 0.20	715	17.6 ±11.46 59.10, 0.20	152	24.45 ±15.12 68.70, 0.30	99	15.32 ±10.41 62.80, 0.20	464
BC	0.54 ±0.42 3.73, 0.02	805	0.55 ±0.52 3.73, 0.04	176	0.85 ±0.50 2.04, 0.02	119	0.47 ±0.40 3.73, 0.03	510
SO_2	1.27 ±1.34 13.93, 0.02	8822	1.2 ±0.99 8.43, 0.20	1981	2.73 ±3.09 13.93, 1.41	1063	1.03 ±0.65 8.43, 0.02	5778
NO_X	2.05 ±1.96 9.86, 0.31	8842	2.37 ±1.33 9.33, 0.65	2001	3.41 ±1.70 9.59, 0.55	1063	1.69 ±0.97 9.33, 0.31	5778
CO	44.78 ±48.03 318.00, 0.20	7822	63.45 ±55.59 318.00, 0.20	1939	104.23 ±54.69 272.40, 0.60	1030	24.68 ±39.91 318.00, 0.20	4853
O_3	50 ±7.86 98.63, 20.43	8817	47.87 ±7.70 67.70, 26.66	2000	49.01 ±10.00 98.63, 20.43	1039	50.53 ±7.56 96.77, 26.66	5778

All data period: 10 Sept.-15 Oct. 2013; Polluted period-1: 18 Sept.-25 Sept. 2013; Polluted period-2: 11 Oct.-15 Oct. 2013

4. Page 24377, lines 5-9, the method for classification of the aerosol types should be briefly introduced, which would be helpful for readers to understand why the particles are categorized as fly ash and others are classified as mineral dust.

Response 4: We briefly introduced the classification.

"For example, mineral dust particles normally display irregular shapes and fly ash particles are spherical, although they both have similar compositions such as Si and Al."

5. Page 24377, line 6 KCl-NaCl particle. The particle should contain K, Na, and Cl in Figure 4.

a) The authors didn't show the crystalline of the particle. The name should be changed to K-Na-Cl.

b) And line 17 organic carbon should be changed to organic.

Response 5 a): We changed the "KCl-NaCl" to K-Na-Cl particle

Response 5 b): We changed the "organic carbon" to "OC".

6. Page 24378, line 25, 33-36 and 34-48 of what? These percentage numbers are in

mass or particle numbers?

Response 6: These percentage numbers are particle numbers.

7. Page 24379, line14 Yak dung,

Response 7: We revised this.

8. Page 24380, line 18, what the regional property is? Please give more specific descriptions.

Response 8: We revised the sentence.

"For example, Du *et al.* (2015) suggested that oxygenated organic aerosols from anthropogenic sources and biomass burning transported over a long distance to the sampling site in the QTP."

9. Page 24380, line 19-20, I do not think primary organic aerosols are refractory. In fact, unlike mineral dust and soot, both are refractory, organic compounds in airborne particles can be completely measured by aerosol mass spectrometer and OC/EC carbon analyzer via heating evaporation, although both instruments can not give molecular information.

Response 9: Thank you. We revised the part.

10. Page 24381, line 10-14, it's better to specifically mark the particles in figures 6, 9 and 10 in order to let readers easily recognize which particle is heterogeneously mixed and which is homogeneously mixed.

Response 10: We specifically point out the heterogeneous and homogeneous mixture. We also added description in each figure caption.

11. Page 24383, line 9-11, this sentence is confusing to me.

Response 11: We revised the sentence as follows:

"However, there is no any report say that the emissions of coal combustion from power plants or other industrial sources have critical regional influence."

12. Page 24383, line 4 and other places throughout the paper, the authors emphasized many times that aerosols in TP are highly aged.

a) What does the age mean?
b) Aerosols in TP are highly aged, if this statement means that aerosols in other East Asia regions are less aged?

Response 12 a): The reviewer 1 also raised this question. We made one definition to explain the "aged" particle in Section 4.3

Response 12 b): We added one sentence here which can make readers to

understand our true meaning. We just pointed out the aged particles in the TP and don't extend to other East Asia regions. Because aging processes of aerosol particles during their transports can significantly change particle hygroscopic and optical properties, we need to pay attention to the issue. In the study we didn't expect the aged particles (SIA associated with fly ash, spherical organic, soot, and mineral) in the remote site. Obviously, the findings in our study in the remote site are different from one recent result in remote Siberia site (Mikhailov et al., 2015).

"Because the complex aerosol particles from different anthropogenic sources intruded into pristine background air, the suspended aerosols became highly aged."

13. In the Figure 4 and Figure 5, EDS spectra were obtained from the individual particles or their part. The measured part on the individual particles should be marked. Otherwise, it's hard for readers to know the details.

Response 13: Thanks. We added markers.

14. In Figure 2/7, equivalent spherical diameter should be equivalent volume diameter.

Response 14: We revised those "spherical" to "volume" in section 2.3 and Figure 2/7.

MS NO.: acp-2015-437

We are grateful for the referee#2' comments. Those comments are all valuable and helpful for improving our paper. We answered the comments carefully and have made corrections in the submitted manuscript. The corrections and the responses are as following:

15. p. 24370, line 11 ". . . at the median pollution level . . ." Both "medium" and "median" are used to indicate the pollution level throughout the text. And "median" also appears as a statistical term in the sections 3.2 and 4.3.

a) To prevent confusion, I suggest using only "medium" for the pollution level. There are other "medians" to be corrected in the line 11 of p. 24378, line 1 of p. 24380, line 2 of p. 24385, and caption of Figure 7.

b) On the contrary, "medium size" in the line 9 of p. 24385 should be "median size".

Response 1 a): We appreciated your comments. We revised the "median" to "medium" in the line 11 of p. 24370, the line 11 of p. 24378, line 1 of p. 24380, line 2 of p. 24385, and caption of Figure 7.

Response 1 b): We revised the "medium size" in the line 9 of p. 24385 to "median size."

16. p. 24371, line 10 "Few aerosol measurements have been conducted in the TP." I do not think the number of the references following this line "few". "Quite a few" sounds more appropriate.

Response 2: Yes, we fully agree with the reviewer. We have revised this sentence as follows:

"Quite a few aerosol measurements have been conducted in the TP".

17. p. 24373, line 14 ". . ., with an atmospheric pressure of 69 kPa, a temperature of 283.5 K, and an assumed particle density of 2 g/cm3."

a) Are the pressure and temperature typical at the sampling site?

b) Also, what kind of particle is assumed that has density of 2 g/cm3?

Response 3 a): The pressure is lower at high altitude but the temperature is

normal in summer.

Response 3 b): We usually used the value to calculate the size cut off of the impactor. We consider ammonium sulfate (1.77 g/cm^3), mineral dust (2.6 g/cm^3), and organic matter (1.5 g/cm^3) as the major aerosol types. The average density (calculated at 1.96) of the mixed aerosol particles was assumed to 2 g/cm3.

18. p. 24375, line 2-6 "Additionally we know the relation . . . diameter smaller than 1 μm." The first sentence is awkward and not grammatically right. How about writing like this? "By plotting the ECD against the ESD (Fig. 2), we also obtain the relationship between them as ESD=0.64ECD." In the following sentence, use the abbreviations (ECD, ESD) provided above. Also, I suggest adding a line like "where the correlation between the ECD and ESD is especially good (Fig.2)." after "diameter smaller than 1 μm".

Response 4: We have revised the sentence as follows:

"By plotting the ECD against the EVD (Fig. 2), we also obtain the relationship between them as EVD=0.64ECD. As a result, ECD (d) of individual aerosol particles measured from the iTEM software can be further converted into EVD (D) based on this relationship. In this study, we only considered fine aerosol particles with equivalent volume diameter smaller than 1 μm where the correlation between the ECD and EVD is especially good (Fig.2)."

19. p. 24377, line 12-14 I suggest deleting the line "because understanding their mixing state enables one to determine their sources,. . ., and potential health effects". This is already mentioned in "Introduction" (p. 24372, line 30).

Response 5: Yes, this is already mentioned in "Introduction". We deleted this sentence.

20. p. 24377, line 14 "TEM observations indicate that SIA and organics . . . normally coated these SIA particles (e.g., Figs. 4d, 5a, and 6)." For readers not familiar with TEM analysis, it would be helpful to briefly explain how the features in the figures can be recognized as SIA particles coated with OC.

Response 6: We added more description.

"In other words, OC occurred on surfaces of the SIA particles."

21. p. 24379, line 8-11 "Because KCl-NaCl particles associated with organic matter . . . saline Qinghai Lake and desert." Here the authors present the reasons why they interpret the KCl-NaCl particles to have resulted from biomass burning. In fact, sea-salt particles (similar to particles from saline lake water) smaller than 1 μm do occur at certain conditions. I prefer a milder expression than "should be excluded", like; "Because the KCl-NaCl particles associated with organic matter occurred only in the short pollution periods and are smaller than typical sea-salt or soil particles (mostly >1μm), it is unlikely that they originated from natural sources such as saline Qinghai Lake and desert."

Response 7: We agreed with your advice, and revised this as follows:

"Because the K-Na-Cl particles associated with organic matter occurred only in the short pollution periods and are smaller than typical sea-salt or soil particles (mostly >1μm), it is unlikely that they originated from natural sources such as saline Qinghai Lake and desert."

22. p. 24379, line 11-15 "In addition, our field experimental investigations . . . in 11-15 October (Du et al., 2015)." The phrase "in addition" repeats in the two successive sentences. The first one had better be deleted.

Response 8: We have revised it as follows:

"Our field experimental investigations showed that a few farmers burned cole flowers and highland barley during the autumn harvest season, which are main season crops in the QTP. In addition, the burning of cow dung for residential heating likely caused the high PM2.5 in 11-15 October (Du et al., 2015)."

23. p. 24379, line 5-15 One thing I'm wondering about the KCl-NaCl particles is that, according to Li et al. (2003), KCl in biomass burning smoke can be converted to K2SO4 or KNO3 pretty rapidly. Li et al. (2003) showed that particles in the smoke 16 km downwind included K2SO4 and KNO3 but not KCl. In the present study, the EDS spectra of the KCl-NaCl particles don't show significant

peak of S (Figure 4), suggesting that the particles are "fresh". Doesn't this mean that the particles came from an area relatively close to the sampling site, rather than were transported for distance?

Response 9: Thank you for your good comments. We also considered the question. First, the area is very clean and the smog plume can be spread quickly following the high wind speed. Therefore, the heterogeneous reactions of KCl with acidic gases could be slow. Second, the agricultural biomass burning spots could exist in large area but different time period. It could be long and short transport distance. In cases, we slightly modified the sentences.

24. p. 24379, line 20-24 "The fly ash-containing particles . . . the background air quality." This part sounds rather enigmatic. Coal combustion emits both fly ash and soot. Why do the proportions of fly ash- and soot-containing particles have a reverse relationship between the high and medium pollution levels? To me, the result seems to indicate that the air at the medium pollution level was more affected by coal combustion than at the high pollution level, and that soot-containing particles at the high pollution level were more from biomass burning than coal combustion. Is this consistent with the authors' other observations?

Response 10: Yes, your understanding is right. Coal combustion should emit more fly ash and organics than soot particles (from our recent results). The coal combustion emissions should constantly influence air quality at the medium level and at the high pollution level. Because biomass burning emissions increase during the high pollution period, coal combustion emissions relatively became smaller.

25. p. 24381, line 4 "The results show that more than 90 % of particles at the background site were highly aged." What kinds of particles are defined as "aged"?

Response 11: Individual particle clearly contained more than two types of components which have been defined above. We added one sentence to define the

aged particles.

"In this study, individual particle clearly containing more than two types of aerosol components (e.g., mineral dust, K-Na-Cl, fly ash, SIA, organics, and soot) has been defined as aged particle. More than 90% of particles at the background site were highly aged."

26. p. 24381, line 16 "Figure 7 shows that SIA with OC coating . . . total individual particles." In Figure 7, "particles with coating" are not shown. So comparison between "coated" and "uncoated" particles cannot be done from the figure.

Response 12: We added explanation. SIA with OC coating represent the particle without inclusions in Figure 7. In Figure 7, we only compared the particle with inclusion and without inclusion.

"SIA with OC coating (i.e., particle without inclusions in Figure 7) shift to one smaller size than the total individual particles."

27. p. 24381, line 25 - p. 24382, line 10 "In addition, Figs. 9 and 10 show . . . within sulfate particles (Adachi et al., 2010)." Here the authors discuss the occurrence of soot inclusions at the surface of SIA particles and their effects on optical absorption. This is one of the most interesting parts of this paper, but I would like to point out that a similar occurrence of soot and sulfate was reported in Posfai et al. (1999) (JGR 104, pages 21685 – 21693). Posfai et al. (1999) suggested that the soot at the edges of sulfate particles is a result of crystallization of the sulfates from droplets on the TEM grids, and that the spatial relationship of soot and sulfates observed on the TEM grids is not the same as that in the original airborne particles (page 21689 of JGR 104). Is there any evidence that can disprove this interpretation?

Response 13: It is very good comment for us to further do more test. Here I would like to answer it. If you noticed that there are not droplets for all the particles on the TEM grids in Figures 9 and 10. Our samples are different from Posfai et al., (1999)' samples collected over ocean. We indeed found the difference using the

same sampler in East China and QTP.

28. p. 24383, line 9-11 “However, the emissions . . . has not been reported.” This sentence is not grammatically right. Please rewrite.

Response 14: We rewrote this sentence as follows:

“However, the emissions of coal combustion from power plants or other industrial sources have a decided regional influence. The statement has not been reported.”

29. p. 24383, line 19-24 “Interestingly, we found that . . . the current climate models.” The same question as I already mentioned for the part in p. 24381-24382. I suppose that the difference in spatial relationship of soot and SIA may be due to relative size of the soot inclusions to the SIA particles. Soot particles observed in polluted areas are much larger than those in remote areas, thus appear to be embedded in sulfates on TEM grids. Isn’t this the case?

Response 15: Here, we try to raise one question based on our study. Soot size is a possible reason for the case. However, the details are beyond this study. We may have one systemic study about soot particles in near future. Indeed, the soot particles have different mixing structure with SIA.

30. p. 24383, line 24-27 “Thirdly, the dominant organics, . . . in fine particles.” I don’t get the meaning of this sentence. Please rewrite.

Response 16: We rewrote this sentence.

“fine aerosol particles in the TP mainly contain organics and sulfates with minor nitrates. The result is largely different from fine particles with high nitrate in more polluted areas (Li et al., 2013a;Du et al., 2015;Xu et al., 2015).”

31. p. 24384, line 3-13 “Fourthly, the high-elevation . . . particle aging and formation in the TP.” Indeed, the atmospheric chemistry and processes in the TP are likely to differ from those in the polluted area. But what kind of differences the present study has revealed? Without discussing the findings from the present study, this part is unnecessary and had better be omitted.

Response 17: We received your advice and deleted this part.

32. p. 24393, Figure 2 caption In the text, the number of the particles analyzed by both AFM and TEM is 194 (p. 24374, line 20). Why is the number in the caption is 157?

Response 18: We made a mistake and revised the 157 to 194.

33. p. 24399, Figure 8 Some of the letters in the figure would be difficult to be read when printed on paper. Enlarge.

Response 19: We enlarge the letters in the figure.

34. Technical corrections:

a) p. 24371, line 3 the brightening and 'dimming' phenomenon

b) p. 24376, line 10 at Waliguan in the summer of 2006, 'that' is . . .

c) p. 24376, line 23 is 'slightly' lower than. . .

d) p. 24381, line 21 by 36-42 % (Fig. '7').

e) p. 24381, line 24 Figure '7' shows that . . .

f) p. 24384, line 13 particle 'aging' and formation . . .

g) p. 24385, line 15 and 'aging' processes of. . .

h) p.24392, Figure 1 caption "Topographical map showing the the sampling location . . ." Delete the second "the".

Response 20: We have revised as follows:

a) Revised "diming" to "dimming" in line 3 of p. 24371

b) We added "that" in the sentence as follows:

That is the site of the observation station of the World Meteorological Organization's (WMO) Global Atmospheric Watch (GAW) (Xue et al., 2011)

c) We revised "slighter" to "slightly".

d) We revised it like this: "Inclusions within SIA particles increase their size by 36-42% (Figure 7)."

e) We revised the number of Figure as follows:

"Figure 7 shows that the number of particles with inclusions increases substantially with diameters above 200 nm."

f) We revised "ageing" to "aging" in the line 13 of p. 24384.

g) We revised “ageing” to “aging” in the line 15 of p. 24385.

h) We deleted the second “the”, the sentence is as follows:

“Topographical map showing the sampling location and surrounding regions in the Tibetan Plateau.”

Mixing state and sources of submicron regional background aerosols in the North Qinghai-Tibetan Plateau and the influence of biomass burning

W.J. Li[1], S.R. Chen[1], Y.S. Xu[2], X. C. Guo[1,2], Y.L. Sun[3], X.Y. Yang[2], Z.F. Wang[3], X.D. Zhao[4], J.M. Chen[1], and W.X. Wang[1,2]

[1]Environment Research Institute, Shandong University, 250100, Jinan, China,

[2]Chinese Research Academy of Environmental Sciences, Beijing 100012, China

[3]State Key Laboratory of Atmospheric Boundary Layer Physics and Atmospheric Chemistry, Institute of Atmospheric Physics, Chinese Academy of Sciences, Beijing 100029, China

[4]Qinghai Environmental Monitoring Center, Qinghai 810007, China.

Correspondence to liweijun@sdu.edu.cn (W.J. Li) and jmchen@sdu.edu.cn (J.M. Chen)

Abstract: Transmission electron microscopy (TEM) was employed to obtain morphology, size, composition, and mixing state of background aerosols with diameter less than 1 μm in the North Qinghai-Tibetan Plateau (QTP) during 15 September to 15 October, 2013. Individual aerosol particles mainly contained secondary inorganic aerosols (SIA-sulfate and nitrate) and organics during clean periods ($PM_{2.5}$ mass concentration less than 2.5 μg/m^3). The presence of K-Na-Cl associated with organics and an increase of soot particles suggest that an intense biomass burning event caused the highest $PM_{2.5}$ concentrations (> 30 μg/m^3) during the study. A large number fraction of the fly ash-containing particles (21.73%) suggests that coal combustion emissions in the QTP significantly contributed to air pollutants at the medium pollution level ($PM_{2.5}$: 10-30 μg/m^3). We concluded that emissions from biomass burning and from coal combustion both constantly contribute to anthropogenic particles in the QTP atmosphere. Based on size distributions of individual particles in different pollution levels, we found that gas condensation on existing particles is an important chemical process for the formation of SIA with organic coating. TEM observations show that refractory aerosols (e.g., soot, fly ash, and visible organic particles) likely adhere to the surface of SIA particles larger than 200 nm due to coagulation. Organic coating and soot on surface of the aged particles likely influence their hygroscopic and optical properties in the QTP, respectively. To our knowledge, this study reports the first microscopic analysis of fine particles in the background QTP air.

1. Introduction

With an immense area (about 2,400,000 km^2) and mean elevation of more than 4000 m above sea level, the Tibetan Plateau (TP), called the ‘‘ridge of the world and third polar”, plays a key role in Asian climatology, especially the formation of monsoons (Lau et al., 2006). Climate on the TP has warmed 0.3 ℃ per decade over the past three decades,, which is twice the rate of observed global warming (Xu et al., 2009). Anthropogenic aerosols and their ice and cloud condensation nuclei (CCN) directly or indirectly leaded to the brightening and dimming phenomenon before and after the 1980s in the TP (You et al., 2010). However, light absorbing carbonaceous aerosol particles (i.e., black carbon (BC) and brown carbon (BrC)) can warm the troposphere (Ramanathan and Carmichael, 2008) and accelerate glacier retreat (Xu et al., 2009). Both the radiative effects of aerosols and their role in cloud forming processes depend on their number, size, chemical properties, and mixing state.

As a consequence, a better understanding of climate change can be achieved by characterizing the TP aerosols. Quite a few aerosol measurements have been conducted in the TP. Ion composition records from a shallow ice core (Zheng et al., 2010) and black soot in the Tibetan glaciers (Xu et al., 2009) both showed that anthropogenic aerosols have increased significantly in the most recent 50 years in the TP. Li et al. (2013a) obtained aerosol components such as 61% mineral, 3% ammonium, 4% nitrate, 18% sulfate, 2% black carbon, and 12% organic matter in $PM_{2.5}$ at a concentration of 21.5 μg m^{-3} during summer of 2010 at Qinghai Lake (36 ℃59`N, 99 ℃54`E; 3200 m a.s.l.) in the northeastern part of the TP. Coal burning and biomass burning were the major sources for anthropogenic aerosols. Xu et al. (2014) showed that the $PM_{2.5}$ mass concentration of 9.5 ± 5.4 μg m^{-3} during a year-long study at the Qilian Shan Station (39.50 ℃N, 96.51 ℃E; 4180 m a.s.l.), a remote site on the northeast edge of the Tibetan Plateau, and their water soluble ionic species were dominated by SO_4^{2-} (39%), CO_3^{2-} (19%), Ca^{2+} (16%), NO_3^- (10%), and NH_4^+ (6%). The study suggests anthropogenic aerosol and natural mineral dust from the Gobi desert together contribute to the particle loading in this remote air. Li et al. (2007) also found anthropogenic ions from residential combustion emissions in precipitation samples at Nam Co station of the central TP. In addition, long-range transport of pollutants from eastern and northwestern China and northern India can contribute black carbon and other air pollutants to the

TP region (Cao et al., 2010;Wang et al., 2010;Engling et al., 2011;Kopacz et al., 2011;Lu et al., 2012;Xu et al., 2013;Zhao et al., 2013;Cong et al., 2015;Duo et al., 2015). Although anthropogenic sources make but a minor contribution to the background TP atmosphere, these anthropogenic aerosols significantly enhanced aerosol optical properties (AOD) in the central and northeastern TP in summer (Cong et al., 2009b;Che et al., 2011;Xia et al., 2011). Therefore, study of the composition and sources of aerosol particles in the TP is necessary to understand their effects on the optical, CCN or IN activity.

The TP has various geographic and natural environmental ecosystems such as mountains, lake basins, deserts, forests, and grasslands. Previous sampling sites have included mountain forests, lake basins , and urban areas in the TP (Li et al., 2007;Che et al., 2011;Engling et al., 2011;Li et al., 2013a;Xu et al., 2014). Grassland is one of the largest geomorphology in the TP. There are only a few herdsmen and farmers living in the vast grasslands of the norther TP. Air pollutants from anthropogenic and natural sources can be easily transported over low bushes in the grasslands under high wind speed in north TP (Figure S1). However, fine aerosols in the troposphere have not been studied over the vast grassland in the northern TP. In this study, we collected samples at a national station of background atmospheric monitoring (NSBAM) on the top of Moshidaban mountain of Menyuan county in Qinghai province (37°35.370′N; 101°17.329′E; elevation: 3295 m), which is within the northern part of the Qinghai-Tibet Plateau (QTP) (Figure 1). The NSBAM is 180 km north of Qinghai Lake (Li et al., 2013a) and 160 km from Waliguan station (Che et al., 2011). Only a few herdsmen live in the grassland but many agricultural activities (e.g., growing hulless barley and rape) mainly occur around Qinghai Lake and Menyuan County.

Although many atmospheric scientists have commented on the probable aerosol impacts on climate and monsoon (Lau et al., 2006), atmospheric observations are still very limited because of the unique geographic and natural environment, electric supply problems, high maintenance costs for instruments, and lack of skilled operators. Because of the immensity of the TP, these previous studies, quite scattered in diverse locations, are insufficient to adequately characterize the aerosols throughout this vast region. In addition, the mixing state of individual particles has not been examined, and only a few studies of particle types and soot have been conducted through electron microcopy (Zhang et al., 2001a;Cong et al., 2009a). Understanding the mixing state of individual particles sheds light on their source, ageing processes, optical, and hygroscopic properties (Posfai

and Buseck, 2010;Li et al., 2015). In the present study, high-resolution transmission electron microscopy (TEM) is employed to study the mixing state and composition of individual submicron particles with diameters < 1 μm. The pollution levels have been evaluated and identified through continuous gaseous and particulate instruments at the sampling site. The anthropogenic sources were further identified based on particle types in the QTP.

2. Experimental methods

2.1 Aerosol sampling

Aerosol particles were collected onto copper TEM grids coated with carbon film (carbon type-B, 300-mesh copper, Tianld Co., China) by a two-stage impactor with a 1-mm-diameter jet nozzle and a 0.5-mm-diameter jet nozzle and an air flow of 1.0 L min^{-1}. Both stages have a 50% collection efficiency, the first at 0.80 μm and the second at 0.20 μm, with an atmospheric pressure of 69 kpa, a temperature of 283.5K, and an assumed particle density of 2 g/cm^3. Sampling times varied from 30 s to 15 min, depending on particle loading. After collection, each sample was placed in a sealed, dry plastic tube and stored in a desiccator at 25 ℃ and 20 ± 3% RH to minimize exposure to ambient air and preserve it for analysis. Altogether, 70 individual samples were collected at the NABAM with the elevation at 3295 m, of which we analyzed the fine particles collected on only the second stage.

2.2 Individual particle analysis

21 aerosol particle samples collected on TEM grids were analyzed with a JEOL JEM-2100 TEM operated at 200 kV. The details about the aerosol collection were marked in Figure 2. Elemental composition was determined semi-quantitatively by using an energy-dispersive X-ray spectrometer (EDS) that can detect elements heavier than C. Cu was excluded from the analyses because the TEM grids are made of Cu. The distribution of aerosol particles on TEM grids was not uniform, with coarser particles occurring near the center and finer particles occurring on the periphery. Therefore, to ensure that the analyzed particles were representative, five areas were chosen from the center and periphery of the sampling spot on each grid. Every particle in the selected area was analyzed. EDS spectra were collected for 15 s in order to minimize radiation exposure and potential beam damage. To better understand the properties of internally mixed

aerosol particles, we also analyzed the composition of different components of individual particles, such as coatings, inclusions, and aggregations. The sampling was controlled to avoid coagulation on the substrate during sampling. The projected areas of individual particles were determined by the iTEM software (Olympus soft imaging solutions GmbH, Germany), the standard image analysis platform for electron microscopy. Altogether 4218 particles in these samples were measured for statistical analyses.

2.3 Particle size measurement

Atomic force microscopy (AFM) with a tapping mode analyzed aerosol particles under ambient conditions. AFM, a digital NanoscopeIIIa Instrument, can detect the three-dimensional morphology of particles. The AFM settings contain imaging forces between 1 and 1.5 nN, scanning rates between 0.5 and 0.8 Hz, and scanning range sizes at 10 μm with a resolution of 512 pixels per length. After the AFM analysis, composition of the same particles was confirmed by TEM, with 194 fine aerosol particles analyzed by this method. The NanoScope analysis software can automatically obtain bearing area (A) and bearing volume (V) of each analyzed particle according to the following formula.

$$A = \pi r^2 = \pi \times \left(\frac{d}{2}\right)^2 = \frac{\pi d^2}{4} \rightarrow \mathrm{d} = \sqrt{\frac{4A}{\pi}} \quad (1)$$

$$V = \frac{4}{3}\pi r^3 = \frac{4}{3} \times \frac{\pi D^3}{8} = \frac{\pi D^3}{6} \rightarrow \mathrm{D} = \sqrt[3]{\frac{6V}{\pi}} \quad (2)$$

Where d is the equivalent circle diameter (ECD) and D is the equivalent volume diameter (EVD). By plotting the ECD against the EVD (Figure 3), we also obtain the relationship between them as EVD=0.64ECD As a result, ECD (d) of individual aerosol particles measured from the iTEM software can be further converted into EVD (D) based on this relationship. In this study, we only considered fine aerosol particles with equivalent volume diameter smaller than 1 μm, where the correlation between the ECD and EVD is especially good (Figure 3).

2.4 FLEXPART particle dispersion model

Air mass history was determined using the Lagrangian particle dispersion model FLEXPART (version 9.02; (Stohl et al., 1998)). FLEXPART simulates the release of thousands of passive tracer air parcels at the specific location, advecting them backwards in

time, providing a representation of the spatial distribution of the air mass at an upwind time referred to as a "retroplume". FLEXPART was driven with 6 h meteorology data from NCEP Climate Forecast System Version 2 (NCEP–CFSv2), including land cover, temperature, relative humidity, and three- dimensional wind, in 37 levels with a resolution of $0.5^{o} \times 0.5^{o}$. In this study, the modeling periods were 72h each simulations and it simulated 4 times each day (beginning at 00:00, 06:00, 12:00, and 18:00, respectively) from 0000 UTC 10 September 2013 to 0000UTC 16 October 2013. Every simulation containing 10000 particles released at the beginning over an altitude range of 3395 m a.s.l to 3995 m a.s.l and the model outputs were recorded every 3-h. The output data of each simulation were combined together to make the figure 1.

2.5 $PM_{2.5}$, trace gases, BC, and meteorological measurements

Thermo TEOM 1405 $PM_{2.5}$ and PM_{10} continually measure the particulate mass concentrations in one-hour averages. Gaseous air pollutants were measured continuously from 1 September to 15 October, 2013: O_3 by a UV photometric analyzer (Teledyne Instruments, Model 400EU); SO_2 by a pulsed UV fluorescence analyzer (M100EU), CO by a non-dispersive infrared analyzer (M300EU), and NO and NO_2 by a commercial chemiluminescence analyzer (M200EU), with the concentrations being recorded in five-minute averages. BC concentrations were measured by an Aethalometer and were recorded in one hour averages. In addition, the non-refractory submicron aerosol species including organics, sulfate, nitrate, ammonium, and chloride were measured in-situ by an Aerodyne Aerosol Chemical Speciation Monitor (ACSM) (Du et al., 2015). Wind direction, wind speed, relative humidity (RH), and temperature were measured and recorded in one hour averages. The time-series meteorological data, shown in Figure S1, and the $PM_{2.5}$ and gaseous concentrations, were provided by the NSBAM.

The average CO mixing ratio is 44.78 ppb at the NSBAM, much lower than the 149 ppb at Waliguan in the summer of 2006, that is the site of the observation station of the World Meteorological Organization's (WMO) Global Atmospheric Watch (GAW) (Xue et al., 2011). This contrast shows that the NSBAM adequately represents background conditions in the expansive grasslands of the northern TP. Time-series concentration variations of six pollutants (i.e., $PM_{2.5}$, BC, SO_2, NO_x, CO, and O_3) show that their highest concentrations occurred from 15 September to 25 September, 2013, and from 11 October to 15 October, 2013, (Figure 2). Therefore, we

considered these two periods as typical high-pollution events. Table 1 shows that five pollutants' concentrations (i.e., $PM_{2.5}$, BC, SO_2, NO_x, and CO) were higher during these pollution events than in the intervening cleaner period; O_3 concentration was close. When the combustion-tracing CO and NO_x concentrations increase, O_3 mixing ratios generally decrease in the QTP due to photochemical consumption (Xue et al., 2011). The primary BC concentrations during the two pollution events were 17% and 81% higher than the intervening cleaner period, respectively (Table 1). $PM_{2.5}$ concentration at 17.06 μg/m^3 at the NSBAM is slightly lower than the 21.5 μg/m^3 in the cleaner Qinghai-lake area in the summer of 2010 (Li et al., 2013a). The air mass back trajectories during the sampling period commonly came from the northwestern TP and crossed the Qinghai-lake area into the northern TP (Figure 1). The air masses during the pollution events adequately represented highly aged and processed long-range transported ambient aerosols in the TP. Figure 2 further displays aerosol collection time under three different $PM_{2.5}$ levels, e.g., $PM_{2.5}$ ≥ 30 μg/m^3, $PM_{2.5}$ between 10-30 μg/m^3, $PM_{2.5}$ < 10 μg/m^3, which represent high pollution level, medium pollution level, and clean pollution level.

3. Results

3.1 Major fine aerosol particles and mixing states

Based on elemental composition and morphology, aerosol particles were classified into six major categories: mineral dust, K-Na-Cl, fly ash, secondary inorganic aerosol (SIA) containing ammoniated sulfates and nitrates, organics, and soot (i.e., BC) (Figures 4-5). For example, mineral dust particles normally display irregular shapes and fly ash particles are spherical, although they both have similar compositions such as Si and Al. This detailed particle classification scheme is described in our previous studies (Li et al., 2014b;Li et al., 2015). The nanosized metal particles which have been frequently detected in ambient aerosols in East China (Li et al., 2013b;Li et al., 2013c) were absent in the Qinghai-Tibet plateau. Mixing properties among the six types of particles were characterized in detail. TEM observations indicate that SIA and organics coexisted in individual fine particles and that organic carbon (OC) coated (e.g., Figures 4d and 5a) or homogeneously mixed (e.g., Figure 6) with these SIA particles. In other words, OC occurred on surfaces of the SIA particles. In addition, we found that many SIA-OC particles had visible inclusions such as mineral dust, fly ash, OC, and soot particles. Identification of the refractory inclusions in internally mixed particles enables one to trace particle sources and their history in the

aging air mass. Their mixing properties consist mostly of SIA-soot-OC (e.g., Figure 4c), SIA-fly ash-soot (e.g., Figure 5d), SIA-fly ash-OC (visible) (e.g., Figure 5d), SIA-fly ash (e.g., Figure 5c), SIA-mineral, SIA-visible OC (e.g., Figure 5a). Therefore, SIA and OC in aerosol particles in the Qinghai-Tibet Plateau were the two most important influences of the mixing state of primary particles.

3.2 Size distribution of aerosol particles

In this section, we describe the size distribution of individual particles with their diameters from 40 nm to 1 μm in different pollution levels. 684 particles collected during clean periods show a median diameter of 230 nm. Figure 7a shows that the size distribution of particles without inclusions determines ambient particle size.

1214 particles during high pollution levels have a median diameter of 260 nm (Figure 7b). Particles with inclusions and particles without inclusions have median diameters of 300 nm and 230 nm, respectively. Figure 7b shows particles with and without inclusions jointly determine the particle size distribution during high pollution levels. We noticed that the size distribution of inclusions in SIA displays a median diameter of 150 nm. A similar pattern of size distribution of 2355 particles occurred in medium pollution levels (Figure 7c). The median diameters of total individual particles, particles with inclusions, particle without inclusions, and inclusions are 290 nm, 340 nm, 250 nm, and 150 nm, respectively. Therefore, the inclusions (e.g., mineral, fly ash, soot, and spherical OC particles) significantly enhanced particle sizes in the background air once they were internally mixed with sulfates.

4. Discussion

4.1 Identification of the pollution events

TEM observations show that individual particle types display large differences under three different $PM_{2.5}$ levels: $\geqslant$ 30 μg/m^3 (high pollution level), 10-30 μg/m^3 (medium pollution level), and $<$ 10 μg/m^3 (clean pollution level) (Figure 3). Aerosol particles collected in clean periods mainly contained SIA and OC. Figure 6 shows that individual SIA particles were commonly coated by OC. Consistently, the ACSM measurement showed that SO_4^{2-} and OC were the main components in PM_1, accounting for 33-36% and 34-48% in mass at the sampling site, respectively (Du et al., 2015). Figure 8 presents the composition of all the analyzed individual particles in the

three pollution levels. In the clean period, we found only a few anthropogenic particles such as fly ash, soot, or their mixed particles with their contributions being less than 10% (Figure 8a).

The increase of KCl and soot particles is suggestive of an intense biomass burning event at the background site (Li et al., 2003). In this study, abundant K-Na-Cl particles and soot-containing particles (e.g., Figure 4) only occurred in pollution period 1 and period 2 which have been indicated as biomass burning (Du et al., 2015). Because the K-Na-Cl particles associated with OC occurred only in the short pollution periods and are smaller than typical sea-salt or soil particles (mostly >1 μm), it is unlikely that they originated from natural sources such as saline Qinghai Lake and desert. Our field experimental investigations showed that a few farmers burned cole flowers and highland barley during the autumn harvest season, which are main season crops in the QTP. In addition, the burning of Yak dung for residential heating likely caused the high $PM_{2.5}$ in 11-15 October (Du et al., 2015).

The distribution of different particle types in the medium pollution level is similar to the high pollution level, except for the absence of K-Na-Cl particles. Figure 8c shows that a large amount of fly ash-containing particles occurred in medium pollution level. Fly ash is generally considered as a reliable fingerprint of coal combustion in residential cooking, power plants, and industrial activities (Li and Shao, 2009). The fly ash-containing particles increase from 11.40% in the high pollution level to 21.73% in the medium one, but soot-containing particles decrease from 38.40% to 25.87%. This result indicates that coal combustion emissions in the QTP significantly affected the background air quality. Compared to individual particles in polluted East China, absence of nanometer metal particles in the QTP suggests that there are no large heavy metal-related industrial emissions in the area under air mass back trajectories (Figure 1). The China Energy Statistical Yearbook of 2013 shows coal combustion occurs in power plants (48.5%), heavy industries (36.4%), and house cooking/heating in rural areas (8.6%) in Qinghai province, particularly nearby the large cities such as Xi'ning (Wen et al., 2013). Although we didn't find any K-Na-Cl particle in the samples under medium pollution level, 50% of SIA (OC coating) and SIA-soot particles containing minor K (Figure 4c-d) frequently occurred in the samples. During long-range transport, once coagulation and condensation of ammoniated sulfates and sulfuric acid in biomass burning particles increase, K-rich particles may transform into sulfur-rich particles with certain amounts of K (Li et al., 2014b). Therefore, SIA particles containing minor K suggest

that biomass burning emissions likely contributed to the QTP aerosols on a more or less constant basis. A similar result has been obtained through the analysis of organic species in $PM_{2.5}$ at Qinghai-lake (Li et al., 2013a). Therefore, we conclude that emissions from biomass burning and from coal combustion significantly contribute to the formation of anthropogenic fine particles in the atmosphere over the QTP.

4.2 Regional effects of biomass burning and industrial emissions

The previous studies proved that trace gases such as SO_2, NO_x, and volatile organic compounds (VOCs) from anthropogenic and natural sources had been transported long distances in the QTP and were transformed into secondary aerosol particles (Xue et al., 2011;Li et al., 2013a;Du et al., 2015;Xu et al., 2015). For example, *Du* et al. (2015) suggested that oxygenated organic aerosols from anthropogenic sources and biomass burning transported over a long distance to the sampling site in the QTP. Because of measurement limitations, there is no research about refractory aerosol particles (e.g., mineral, fly ash, and soot) in fine particles and primary organic particles. In contrast, TEM observations can adequately characterize these refractory particles internally mixed with SIA based on their unique morphology and composition (Figures 4-5). We identified abundant refractory particles at the three pollution levels at the regional background site. Therefore, the nanosized refractory particles and trace gases from various anthropogenic sources including biomass burning can together be transported long distances. The FLEXPART simulation shows that these anthropogenic particles mainly originated from biomass burning between the Qinghai lake and Menyuan county and heavy industries and coal-fired power plants in western areas of Xining city (Figure 1).

4.3 Mixing mechanisms of aged aerosol particles

In this study, individual particle clearly containing more than two types of aerosol components (e.g., mineral dust, K-Na-Cl, fly ash, SIA, organics, and soot) has been defined as aged particle. More than 90% of particles at the background site were highly aged. SIA with OC coating were the dominant particles and could determine the hygroscopic properties of the ambient aerosol particles. OC coatings on inorganic particles can induce an early deliquescence of particle surface compared to that of the pure inorganic compounds (Li et al., 2014a). Recently, Mikhailov et al. (2015) found that the semi-solid state of the OC coating can lead to kinetic limitations of water uptake and release during hydrate and dehydrate cycles in the background area. OC dominated in

298 fine particles, accounting for 43% of mass on average, followed by sulfate (28%) and nitrate (1%)
299 (Du et al., 2015). TEM observations further indicated that OC can heterogeneously and
300 homogeneously be mixed with all the fine SIA particles (Figures 6, 9-10). This finding is in
301 agreement with the study of new particle formation and growth events during the sampling period,
302 in which oxygenated organics significantly contributed into particle growth in the QTP (Du et al.,
303 2015). SIA with OC coating (i.e., particle without inclusions in Figure 7) shift to one smaller size
304 than the total individual particles. Gas condensation on the existing particles is an important
305 chemical process for formation of SIA with OC coating. Therefore, OC coating of the aged
306 aerosol particles is likely an important factor to determine particle hygroscopic growth and phase
307 transitions in the QTP.

308 Inclusions within SIA particles increase their size by 36-42% (Figure 7). The size distribution
309 of individual particles shows that particles without inclusions have a median size of 200 nm - 250
310 nm at the background site. Figure 7 shows that the number of particles with inclusions increases
311 substantially with diameters above 200 nm. In addition, Figures 9-10 show soot, fly ash, and
312 visible OC particles likely adhere to the surface of SIA particles, which is different from many
313 refractory particles embedded within SIA particles in East China (Li and Shao, 2009;Li et al.,
314 2011b;Li et al., 2014b). Therefore, the coagulation process between primary refractory particles
315 and SIA particles with diameters > 200 nm could be dominant in the atmosphere. The results are
316 different from the background aerosol particles in Siberia where these soot, fly ash and visible OC
317 particles are absent (Mikhailov et al., 2015). In particular, the mixing structure of soot on the
318 surface of SIA particles is different from the previous studies (Li et al., 2003;Adachi et al.,
319 2010;Li et al., 2015). Therefore, sulfates cannot act as the lens to enhance optical absorption of
320 soot particles before individual particles totally deliquesces in humid air (Ramanathan and
321 Carmichael, 2008). Light absorption of soot on surfaces of sulfate particles have 30% lower than
322 soot centered within sulfate particles (Adachi et al., 2010). We found that number of
323 soot-containing particles increase during the biomass burning periods (Figure 8b-c). Also, Figure 3
324 shows that the BC concentrations exceeded 1.0 μg m^{-3} during biomass burning periods which is
325 two times higher than the average value during the sampling period. As a result, large amounts of
326 soot particles from biomass burning in background atmosphere likely change atmospheric optical
327 absorption and modify optical feedback of ice/snow after their deposition in the QTP (Che et al.,

2011;Ming et al., 2012). The microstructure of soot particles can improve understanding of the optical properties of fine aerosol particles and better evaluate their climate impacts using climate models.

We also notice that a large number of particles without inclusions can occur with diameters > 300 nm, although the particle numbers decrease (Figure 7). TEM observations reveal distinct rims on some larger particles, as the examples shown in Figures 5a, 5d, 9b, 10a. Our previous studies showed that the cloud and fog residues on the substrate can display distinct rims (Kojima et al., 2004;Li et al., 2011a;Li et al., 2011b). Therefore, these large particles with distinct rims probably undergo complicated atmospheric transformation such as cloud/fog processing during their growth. Briefly, our study indicates that aerosol particles in different size regimes have different atmospheric chemical or physical processes in the background air over the QTP.

4.4 Further considerations about fine particles over Qinghai-Tibetan plateau

Emissions from coal combustion and biomass burning contribute fine particles into the background air over the QTP. Because the complex aerosol particles from different anthropogenic sources intruded into pristine background air, the suspended aerosols became highly aged. Because of the sensitive feedback of climate in the TP, these aged aerosol particles in the plateau become particularly interesting. Firstly, transport and sources of aerosol particles should be evaluated, and, indeed, most studies in the TP have accomplished this (Cong et al., 2009a;Cong et al., 2009b;Engling et al., 2011;Lu et al., 2012;Du et al., 2015;Xu et al., 2015). These studies all suggested that long-range transport of fine particles from biomass burning and other anthropogenic sources (cooking and vehicular emissions) often reach the TP. However, the emissions of coal combustion from power plants or other industrial sources have a decided regional influence. The statement has not been reported. Our studies provide new evidence that fly ash particles serve as a reliable fingerprint of coal-combustion at the background site. Following economic development in western China, coal combustion increases, chiefly for electrical power generation and other industrial activities (Figure S2). Secondly, highly aged particles such as ambient aerosols and CCN in the atmosphere and sediment in ice/snow can directly or indirectly impact on climate in the TP (Cong et al., 2009b;You et al., 2010;Che et al., 2011;Lu et al., 2012;Ming et al., 2012;He et al., 2014;Wang et al., 2015;Yang et al., 2015). At the background sampling site the mean BC concentration was 0.54 μg/m^3. Interestingly, we found that most fine

soot (BC) particles adhere to individual SIA (Figures 9-10) in the Qinghai plateau while many soot particles were embedded within SIA in polluted areas of East China (Li and Shao, 2009;Li et al., 2011b). The detailed physical properties (e.g., mixing structure and size) of soot in air and ice/snow should be further studied in the TP, which can improve the current climate models. Thirdly, fine aerosol particles in the TP mainly contain OC and sulfates with minor nitrates. The result is largely different from fine particles with high nitrate in more polluted areas (Li et al., 2013a;Du et al., 2015;Xu et al., 2015). Although regional transport from anthropogenic sources or biomass burning significantly increase particle concentrations, mineral dust from surrounding deserts and organics from plants are still dominant in the TP throughout the year (Zhang et al., 2001b;Wang et al., 2010;Li et al., 2013a;Xu et al., 2014).

5. Conclusions

Time-series of six pollutants ($PM_{2.5}$, BC, SO_2, NO_x, CO, and O_3) were obtained at a national station of background atmospheric monitoring (NSBAM) on the top of Moshidaban Mountain in the North QTP during 15 September – 15 October, 2013. The mean concentrations of $PM_{2.5}$, BC, SO_2, NO_x, CO, and O_3 were 17.06 μg/m^3, 0.54 μg/m^3, 1.27 ppb, 2.05 ppb, 44.78 ppb, and 50.00 ppb, respectively. TEM was employed to study individual fine particles with the diameter less than 1 μm that were classified into six major particle types: mineral dust, K-Na-Cl, fly ash, secondary inorganic aerosol (SIA) containing ammoniated sulfates and nitrates, organics, soot (i.e., BC). Individual fine particle types display large differences under three different $PM_{2.5}$ levels: $PM_{2.5} \geq 30$ μg/m^3 (high pollution level), $10 \leq PM2.5 < 30$ μg/m^3 (medium pollution level), and < 10 μg/m^3 (clean period). Individual fine particles in clean periods mainly contained SIA and organics. The presence of K-Na-Cl coated by organics and increased soot particles during high pollution levels suggests an intense biomass burning event near the background site. Large amounts of fly ash-containing particles occurred in medium pollution level. The fly ash-containing particles increased from 11.40% at the medium pollution level to 21.73% at the high pollution level, but soot-containing particles decreased from 38.40% to 25.87%. This result indicates that coal combustion emissions in the QTP significantly affected the background air quality. In addition, SIA particles containing minor K suggest that biomass burning emissions were a constant contributor to aerosol particles in the QTP. We concluded that the emissions from

biomass burning and coal-used anthropogenic activities contribute anthropogenic particles into the QTP atmosphere.

Aerosol particles containing SIA core and OC coating display smaller median size than the total particles. Gas condensation on the particles is an important chemical process for their formation. The number concentration of particles with inclusions increased markedly above 200 nm. TEM observations show that refractory aerosols (e.g., soot, fly ash, and visible organic particles) likely adhere to the surface of SIA particles, suggesting physical coagulation could be dominant in background air. These results notably improve our understanding of sources and aging processes of long-range transported aerosols in the QTP. The transport of these aerosol particles, as well as their, hygroscopic, and optical properties and atmospheric chemistry, require further study in the TP.

Author contribution*:* W.J.L. and J.M.C. designed the research and wrote the paper; W.J.L. and S.R.C. carried TEM and AFM experiments; Y.S.X., X.C.G., Y.L.Y., and X.Y.Y. conducted field experiments; X.D.Z provided the online monitoring data; Y.S.X, J.M.C., Z.F.W., and W.X.W lead the projects.

Acknowledgements. We appreciate Peter Hyde's comments and proofreading. We are grateful to Yong Ren for processing FLEXPART data for figure 1**.** This work was supported by the National Natural Science Foundation of China (41575116 and 41375133), Shandong Provincial Science Fund for Distinguished Young Scholars, China (JQ201413), Young Scholars Program of Shandong University (2015WLJH37), Taishan Scholars (ts20120522), Fundamental Research Funds of Shandong University (2014QY001), and State Key Laboratory of Atmospheric Boundary Layer Physics and Atmospheric Chemistry (LAPC-KF-2014-03).

References

Adachi, K., Chung, S. H., and Buseck, P. R.: Shapes of soot aerosol particles and implications for their effects on climate, J. Geophys. Res., 115, doi:10.1029/2009JD012868, 2010.

Cao, J., Tie, X., Xu, B., Zhao, Z., Zhu, C., Li, G., and Liu, S.: Measuring and modeling black carbon (BC) contamination in the SE Tibetan Plateau, J. Atmos. Chem., 67, 45-60, 2010.

Che, H., Wang, Y., and Sun, J.: Aerosol optical properties at Mt. Waliguan Observatory, China, Atmos. Environ., 45, 6004-6009, 2011.

Cong, Z., Kang, S., Dong, S., and Zhang, Y.: Individual particle analysis of atmospheric aerosols at Nam Co, Tibetan Plateau, Aerosol Air Qual. Res., 9, 323-331, 2009a.

Cong, Z., Kang, S., Smirnov, A., and Holben, B.: Aerosol optical properties at Nam Co, a remote site in central Tibetan Plateau, Atmos. Res., 92, 42-48, 2009b.

Cong, Z., Kawamura, K., Kang, S., and Fu, P.: Penetration of biomass-burning emissions from South Asia through the Himalayas: new insights from atmospheric organic acids, Sci. Rep., 5, DOI: 10.1038/srep09580, 2015.

Du, W., Sun, Y. L., Xu, Y. S., Jiang, Q., Wang, Q. Q., Yang, W., Wang, F., Bai, Z. P., Zhao, X. D., and Yang, Y. C.: Chemical characterization of submicron aerosol and particle growth events at a national background site (3295 m a.s.l.) in the Tibetan Plateau, Atmos. Chem. Phys. Discuss., 15, 13515-13550, 2015.

Duo, B., Zhang, Y., Kong, L., Fu, H., Hu, Y., Chen, J., Li, L., and Qiong, A.: Individual particle analysis of aerosols collected at Lhasa City in the Tibetan Plateau, J. Environ. Sci., 29, 165-177, 2015.

Engling, G., Zhang, Y.-N., Chan, C.-Y., Sang, X.-F., Lin, M., Ho, K.-F., Li, Y.-S., Lin, C.-Y., and Lee, J. J.: Characterization and sources of aerosol particles over the southeastern Tibetan Plateau during the Southeast Asia biomass-burning season, Tellus B, 63, 117-128, 10.1111/j.1600-0889.2010.00512.x, 2011.

He, C., Li, Q., Liou, K.-N., Takano, Y., Gu, Y., Qi, L., Mao, Y., and Leung, L. R.: Black carbon radiative forcing over the Tibetan Plateau, Geophy. Res. Lett., 41, 2014GL062191, 2014.

Kojima, T., Buseck, P. R., Wilson, J. C., Reeves, J. M., and Mahoney, M. J.: Aerosol particles from tropical convective systems: Cloud tops and cirrus anvils, J. Geophys. Res., 109, 12201-12201, 2004.

Kopacz, M., Mauzerall, D. L., Wang, J., Leibensperger, E. M., Henze, D. K., and Singh, K.: Origin and radiative forcing of black carbon transported to the Himalayas and Tibetan Plateau, Atmos. Chem. Phys., 11, 2837-2852, 2011.

Lau, K. M., Kim, M. K., and Kim, K. M.: Asian summer monsoon anomalies induced by aerosol direct forcing: the role of the Tibetan Plateau, Clim Dyn, 26, 855-864, 2006.

Li, C., Kang, S., Zhang, Q., and Kaspari, S.: Major ionic composition of precipitation in the Nam Co region, Central Tibetan Plateau, Atmos. Res., 85, 351-360, 2007.

Li, J., Posfai, M., Hobbs, P. V., and Buseck, P. R.: Individual aerosol particles from biomass burning in southern Africa: 2, Compositions and aging of inorganic particles, J. Geophys. Res., 108, doi:10.1029/2002JD002310, 2003.

Li, J. J., Wang, G. H., Wang, X. M., Cao, J. J., Sun, T., Cheng, C. L., Meng, J. J., Hu, T. F., and Liu, S. X.: Abundance, composition and source of atmospheric PM 2.5 at a remote site in the Tibetan Plateau, China, Tellus B, 65, 10.3402/tellusb.v65i0.20281, 2013a.

Li, W., Li, P., Sun, G., Zhou, S., Yuan, Q., and Wang, W.: Cloud residues and interstitial aerosols from non-precipitating clouds over an industrial and urban area in northern China, Atmos. Environ., 45, 2488-2495, 2011a.

Li, W., Wang, T., Zhou, S., Lee, S., Huang, Y., Gao, Y., and Wang, W.: Microscopic Observation of Metal-Containing Particles from Chinese Continental Outflow Observed from a Non-Industrial Site, Environ. Sci. Technol., 47, 9124-9131, 2013b.

Li, W., Wang, Y., Collett, J. L., Chen, J., Zhang, X., Wang, Z., and Wang, W.: Microscopic Evaluation of Trace Metals in Cloud Droplets in an Acid Precipitation Region, Environ. Sci. Technol., 47, 4172-4180, 2013c.

Li, W., Chi, J., Shi, Z., Wang, X., Chen, B., Wang, Y., Li, T., Chen, J., Zhang, D., Wang, Z., Shi, C., Liu, L., and Wang, W.: Composition and hygroscopicity of aerosol particles at Mt. Lu in South China: Implications for acid precipitation, Atmos. Environ., 94, 626-636, http://dx.doi.org/10.1016/j.atmosenv.2014.06.003, 2014a.

Li, W., Shao, L., Shi, Z., Chen, J., Yang, L., Yuan, Q., Yan, C., Zhang, X., Wang, Y., Sun, J., Zhang, Y., Shen, X., Wang, Z., and Wang, W.: Mixing state and hygroscopicity of dust and haze particles before leaving Asian continent, J. Geophys. Res., 119, 1044-1059, 2014b.

Li, W., Shao, L., Zhang, D., Ro, C.-U., Hu, M., Bi, X., Geng, H., Matsuki, A., Niu, H., and Chen, J.: A review of single aerosol particle studies in the atmosphere of East Asia: morphology, mixing state, source, and heterogeneous reactions, J. Clean. Prod., DOI:10.1016/j.jclepro.2015.1004.1050 (in press), 2015.

Li, W. J., and Shao, L. Y.: Transmission electron microscopy study of aerosol particles from the brown hazes in northern China, J. Geophys. Res., 114, doi:10.1029/2008JD011285, 2009.

Li, W. J., Zhou, S. Z., Wang, X. F., Xu, Z., Yuan, C., Yu, Y. C., Zhang, Q. Z., and Wang, W. X.: Integrated evaluation of aerosols from regional brown hazes over northern China in winter: Concentrations, sources, transformation, and mixing states, J. Geophys. Res., 116, doi:10.1029/2010JD015099, 2011b.

Lu, Z., Streets, D. G., Zhang, Q., and Wang, S.: A novel back-trajectory analysis of the origin of black carbon transported to the Himalayas and Tibetan Plateau during 1996-2010, Geophy. Res. Lett., 39, L01809, 10.1029/2011gl049903, 2012.

Mikhailov, E. F., Mironov, G. N., Pöhlker, C., Chi, X., Krüger, M. L., Shiraiwa, M., Förster, J. D., Pöschl, U., Vlasenko, S. S., Ryshkevich, T. I., Weigand, M., Kilcoyne, A. L. D., and Andreae, M. O.: Chemical composition, microstructure, and hygroscopic properties of aerosol particles at the Zotino Tall Tower Observatory (ZOTTO), Siberia, during a summer campaign, Atmos. Chem. Phys., 15, 8847-8869, 10.5194/acp-15-8847-2015, 2015.

Ming, J., Du, Z., Xiao, C., Xu, X., and Zhang, D.: Darkening of the mid-Himalaya glaciers since 2000 and the potential causes, Environ. Res. Lett., 7, 014021, 10.1088/1748-9326/7/1/014021, 2012.

Posfai, M., and Buseck, P. R.: Nature and Climate Effects of Individual Tropospheric Aerosol Particles, Annu. Rev. Earth Pl. Sc., 38, 17-43, 2010.

Ramanathan, V., and Carmichael, G.: Global and regional climate changes due to black carbon, Nature Geosci, 1, 221-227, 2008.

Stohl, A., Hittenberger, M., and Wotawa, G.: Validation of the lagrangian particle dispersion model FLEXPART against large-scale tracer experiment data, Atmos. Environ., 32, 4245-4264, http://dx.doi.org/10.1016/S1352-2310(98)00184-8, 1998.

Wang, Q. Y., Huang, R. J., Cao, J. J., Tie, X. X., Ni, H. Y., Zhou, Y. Q., Han, Y. M., Hu, T. F., Zhu, C. S., Feng, T., Li, N., and Li, J. D.: Black carbon aerosol in winter northeastern Qinghai-Tibetan Plateau, China: the effects from South Asia pollution, Atmos. Chem. Phys. Discuss., 15, 14141-14169, 2015.

Wang, X., Huang, J., Zhang, R., Chen, B., and Bi, J.: Surface measurements of aerosol properties over northwest China during ARM China 2008 deployment, J. Geophys. Res., 115, doi:10.1029/2009JD013467, 2010.

Wen, J., Meng, H., Wang, X., and coauthors: China Energy Statistical Yearbook, Department of Energy Statistics, National Bureau of Statistics, People's Republic of China, Beijing, 1-355, 2013.

Xia, X., Zong, X., Cong, Z., Chen, H., Kang, S., and Wang, P.: Baseline continental aerosol over the central Tibetan plateau and a case study of aerosol transport from South Asia, Atmos. Environ., 45, 7370-7378, 2011.

Xu, B., Cao, J., Hansen, J., Yao, T., Joswia, D. R., Wang, N., Wu, G., Wang, M., Zhao, H., Yang, W., Liu, X., and He, J.: Black soot and the survival of Tibetan glaciers, Proc. Natl. Acad. Sci. U.S.A., 106, 22114-22118, 2009.

Xu, J., Zhang, Q., Li, X., Ge, X., Xiao, C., Ren, J., and Qin, D.: Dissolved Organic Matter and Inorganic Ions in a Central Himalayan Glacier—Insights into Chemical Composition and Atmospheric Sources, Environ. Sci. Technol., 47, 6181-6188, 2013.

Xu, J., Wang, Z., Yu, G., Qin, X., Ren, J., and Qin, D.: Characteristics of water soluble ionic species in fine particles from a high altitude site on the northern boundary of Tibetan Plateau: Mixture of mineral dust and anthropogenic aerosol, Atmos. Res., 143, 43-56, 2014.

Xu, J. Z., Zhang, Q., Wang, Z. B., Yu, G. M., Ge, X. L., and Qin, X.: Chemical composition and size distribution of summertime PM2.5 at a high altitude remote location in the northeast of the Qinghai–Xizang (Tibet) Plateau: insights into aerosol sources and processing in free troposphere, Atmos. Chem. Phys., 15, 5069-5081, 2015.

Xue, L. K., Wang, T., Zhang, J. M., Zhang, X. C., Deliger, Poon, C. N., Ding, A. J., Zhou, X. H., Wu, W. S., Tang, J., Zhang, Q. Z., and Wang, W. X.: Source of surface ozone and reactive nitrogen speciation at Mount Waliguan in western China: New insights from the 2006 summer study, J. Geophys. Res., 116, doi:10.1029/2010JD014735, 2011.

Yang, S., Xu, B., Cao, J., Zender, C. S., and Wang, M.: Climate effect of black carbon aerosol in a Tibetan Plateau glacier, Atmos. Environ., 111, 71-78, 2015.

You, Q., Kang, S., Flügel, W.-A., Sanchez-Lorenzo, A., Yan, Y., Huang, J., and Martin-Vide, J.: From brightening to dimming in sunshine duration over the eastern and central Tibetan Plateau (1961–2005), Theor. Appl. Climatol., 101, 445-457, 2010.

Zhang, D., Iwasaka, Y., and Shi, G.: Soot particles and their impacts on the mass cycle in the Tibetan atmosphere, Atmos. Environ., 35, 5883-5894, 2001a.

Zhang, X. Y., Arimoto, R., Cao, J. J., An, Z. S., and Wang, D.: Atmospheric dust aerosol over the Tibetan Plateau, J. Geophys. Res., 106, 18471-18476, 2001b.

Zhao, Z., Cao, J., Shen, Z., Xu, B., Zhu, C., Chen, L. W. A., Su, X., Liu, S., Han, Y., Wang, G., and Ho, K.: Aerosol particles at a high-altitude site on the Southeast Tibetan Plateau, China: Implications for pollution transport from South Asia, J. Geophys. Res., 118, 11,360-311,375, 2013.

Zheng, W., Yao, T., Joswiak, D. R., Xu, B., Wang, N., and Zhao, H.: Major ions composition records from a shallow ice core on Mt. Tanggula in the central Qinghai-Tibetan Plateau, Atmos. Res., 97, 70-79, 2010.

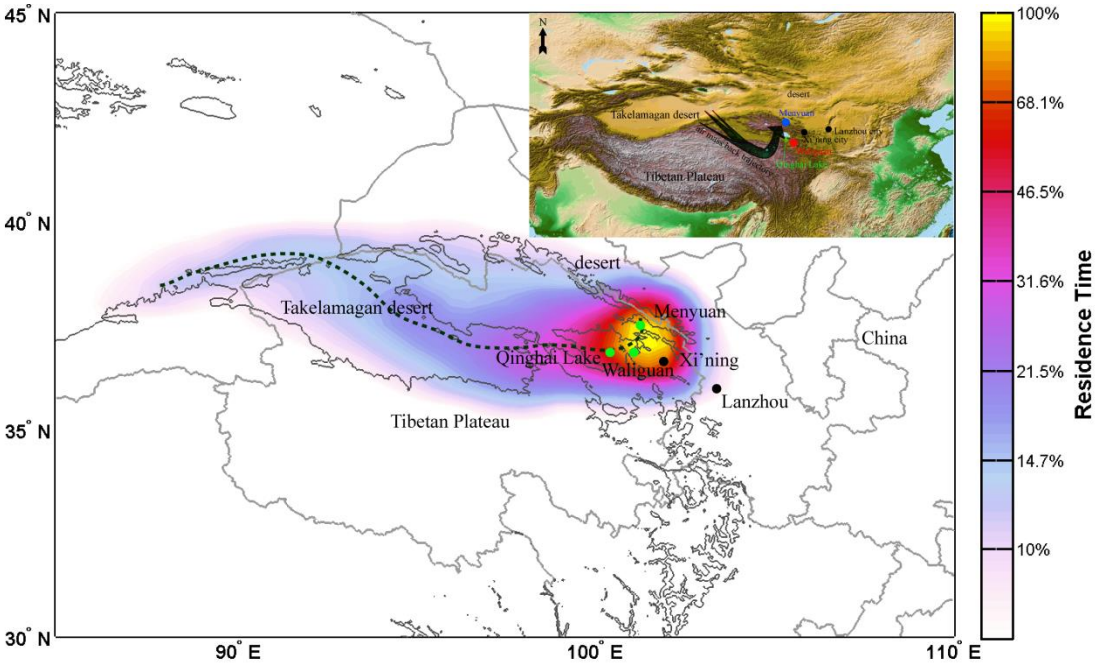

Figure 1 FLEXPART retroplume simulations during 10 September-15 October. Topographical map showing the sampling location and surrounding regions in the Tibetan Plateau. Xi'ning is the caption city of Qinghai province. Menyuan represents sampling site. The black line shows the major back trajectories of air mass during 10 September - 15 October, 2013 based on the spatial distribution of the air mass. The main air mass mainly passed through rural areas, grasslands, and desert.

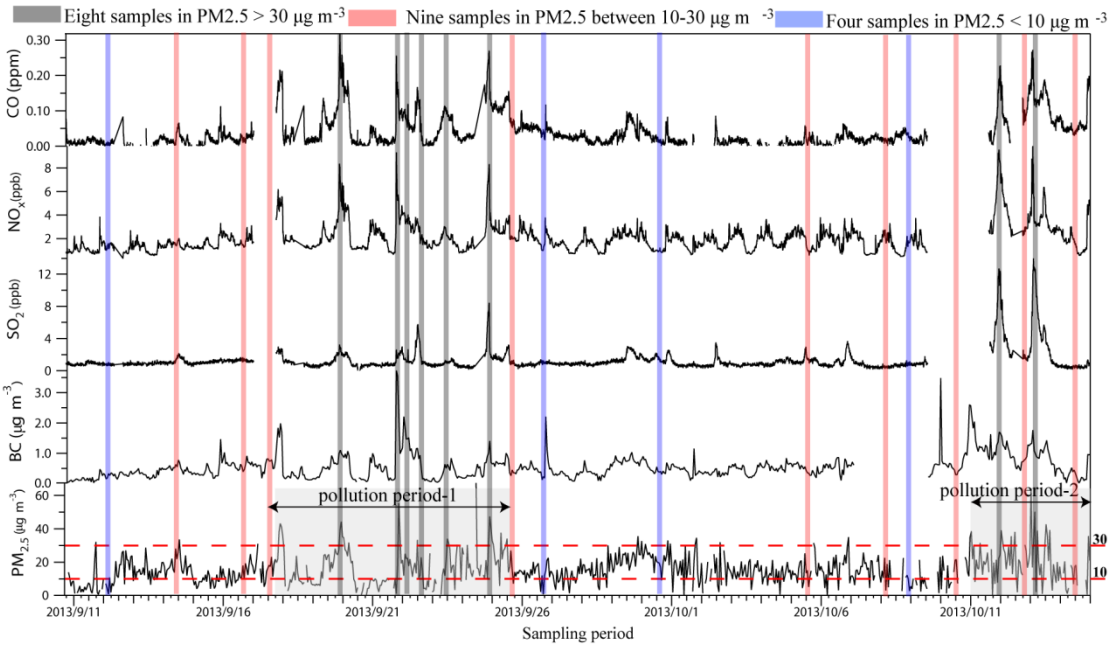

Figure 2 Time-series concentration of air pollutants (i.e., CO, NO_x, SO_2, BC, and $PM_{2.5}$) during 11 September – 15 October, 2013. The sampling time was marked by grey column ($PM_{2.5} \geq 30$ $\mu g/m^3$), pink column ($PM_{2.5}$ between 10-30 $\mu g/m^3$), blue column ($PM_{2.5} < 10$ $\mu g/m^3$).

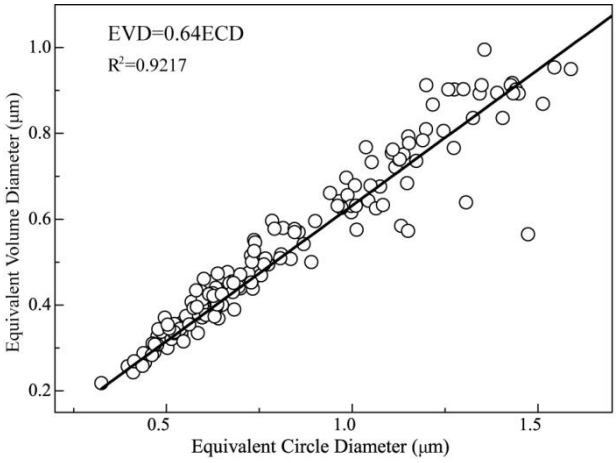

Figure 3 Correction of equivalent circle diameters (ECD) vs equivalent volume diameter (EVD) of 194 aerosol particles.

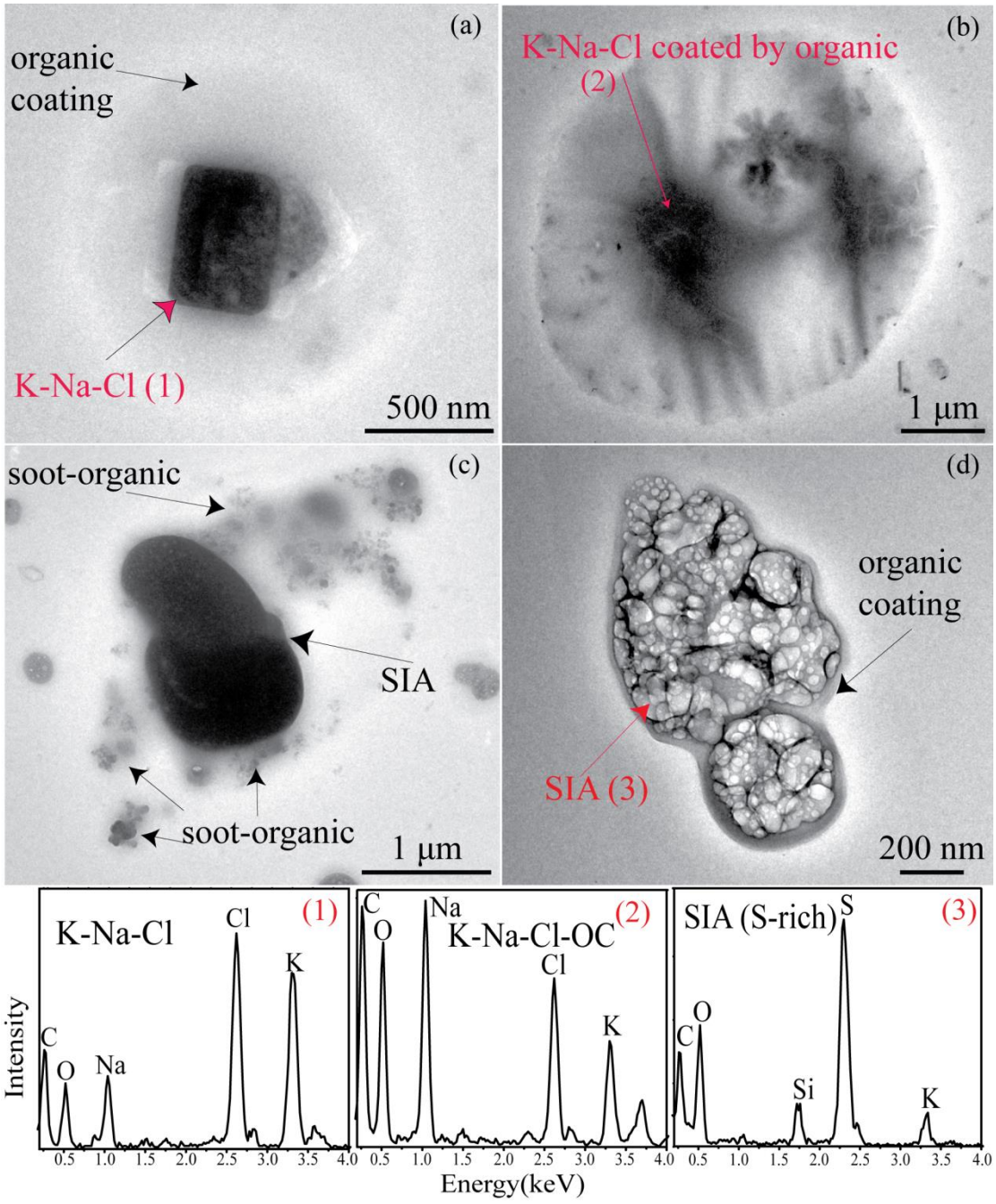

Figure 4 TEM images of (a-b) K-Na-Cl particle with organic coating on 22 September and 13 October. (c) SIA-soot with organic coating on 22 September. (d) SIA with organic coating on 11 October. EDS spectra shows elemental compositions of each particle type in each TEM image.

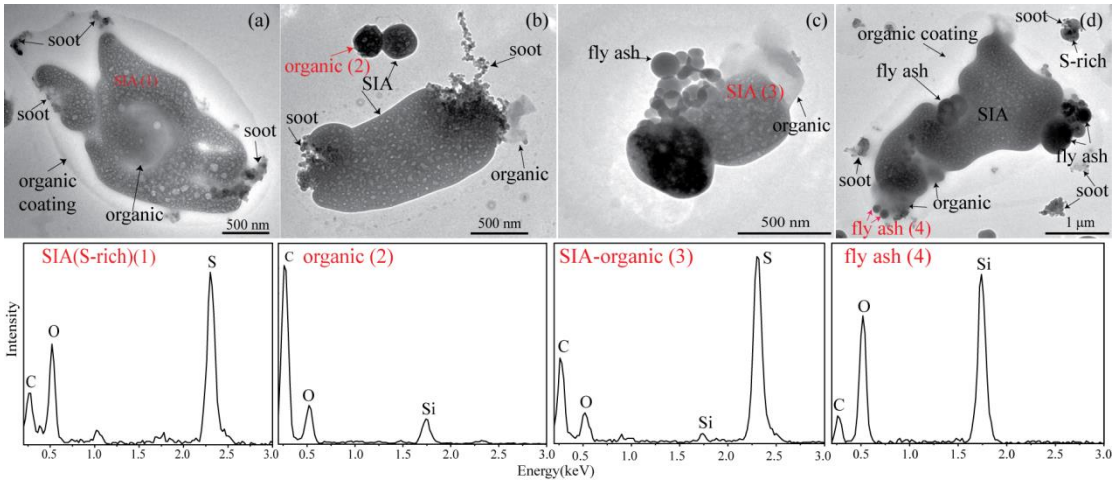

Figure 5 TEM images of (a) SIA-soot-OC (visible) with organic coating on 16 September. (b) SIA-soot-OC on 14 September. (c) SIA-fly ash-OC on 5 October. (d) SIA-fly ash-soot-OC (visible) with organic coating on 16 September. EDS spectra shows elemental composition of each particle type in each TEM image.

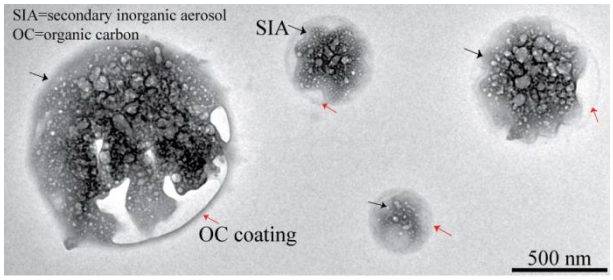

Figure 6 TEM image of individual particles collected in clean period with $PM_{2.5}$ mass concentration less than 10 μg/m^3. SIA particles tend to homogeneously mix with organics.

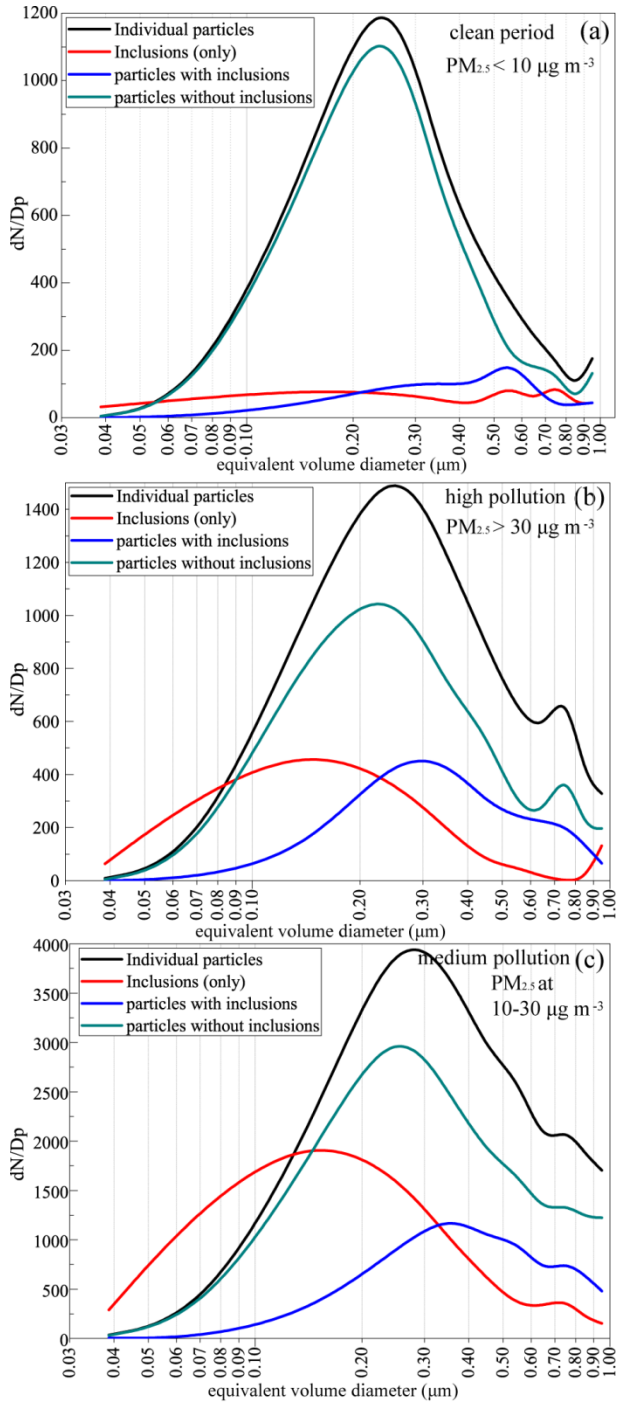

Figure 7 Size distributions of individual particles, inclusions, particles with inclusions, and particles without inclusions. (a) Clean periods under $PM_{2.5}$ at 10 μg/m^3. (b) The high pollution level under $PM_{2.5}$ larger than 30 μg/m^3. (c) The medium pollution level under $PM_{2.5}$ among 10 μg/m^3 - 30 μg/m^3.

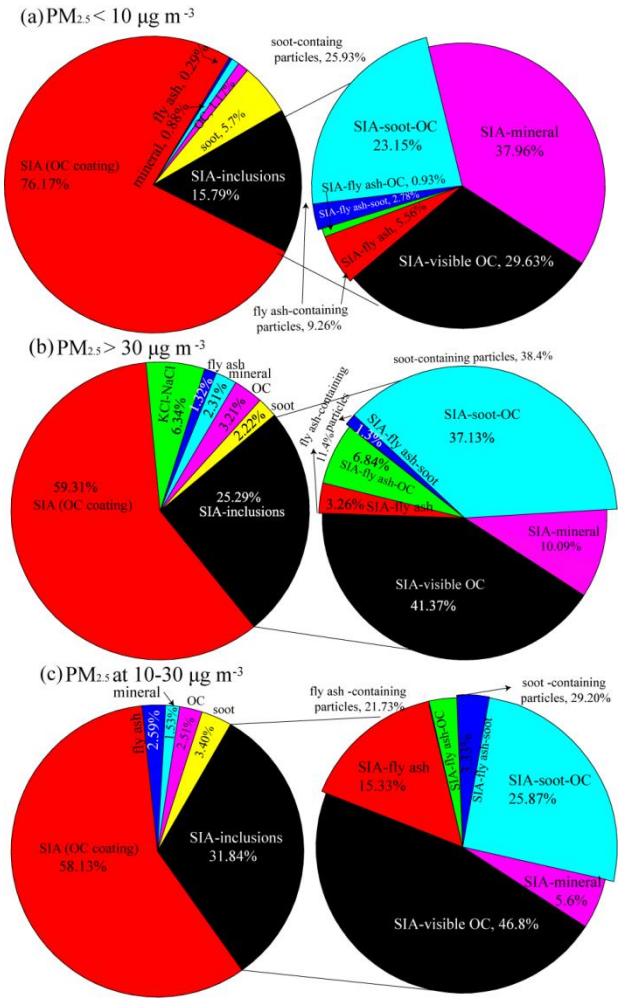

Figure 8 Identification of the pollution events based on individual particle analysis (a) 684 individual particles and 108 SIA-inclusion particles. (b) 1214 individual particles and 307 SIA-inclusion particles. Eight samples were collected in $PM_{2.5}$ larger than 30 μg m^{-3} induced by biomass burning emission. (c) 2355 individual particles and 750 SIA-inclusion particles. Nine samples were collected in $PM_{2.5}$ at the range of 10-30 μg m^{-3} induced by biomass burning and industrial emissions. Four samples were collected in $PM_{2.5}$ smaller than 10 μg m^{-3} which indicates clean period.

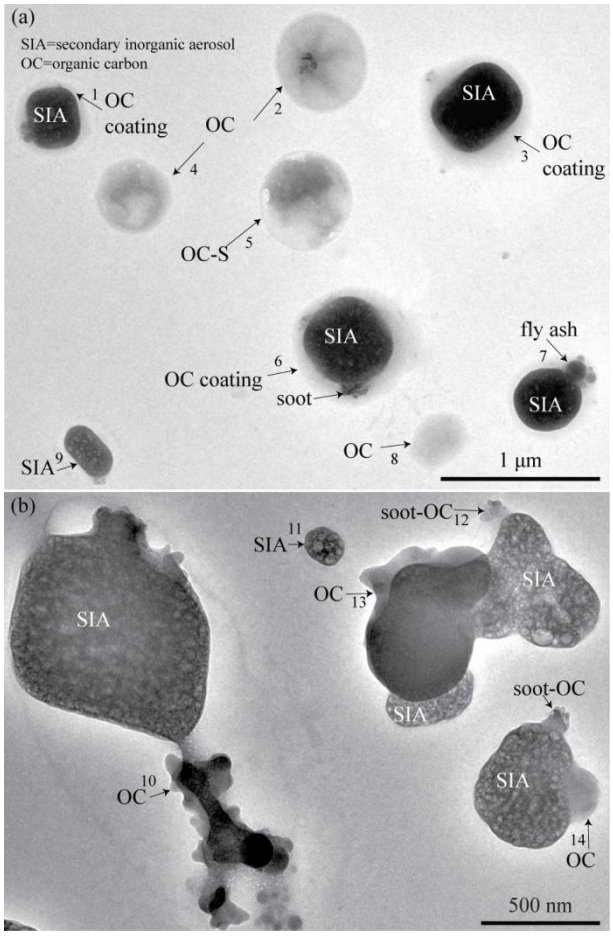

Figure 9 Individual particles during biomass burning periods with $PM_{2.5}$ mass concentration larger than 30 μg/m^3. (a) OC and SIA-soot-(OC coating) particles on 12 October. (b) SIA-soot-(visible OC) on 19 October. OC in particles 1, 3, 6, 10, 13, 14 are heterogeneously mixed with SIA particles and particles 2, 4, 5, 8 homogeneously mixed with minor SIA.

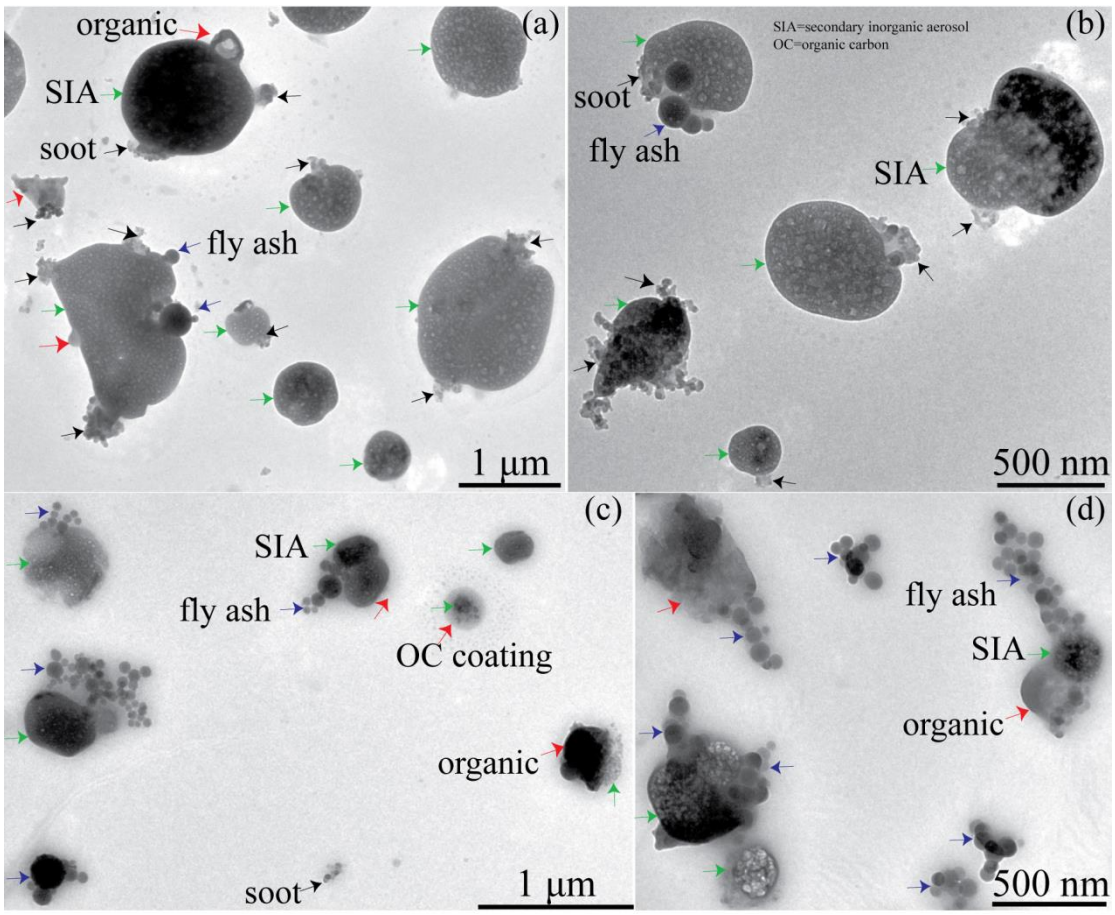

Figure 10 Individual particles collected under $PM_{2.5}$ mass concentration among 10-30 μg/m^3. (a) Mixture of SIA and soot, fly ash particles collected on 14 September. (b) Mixture of SIA and soot, fly ash particles collected on 18 September. (c) Mixture of SIA and fly ash, soot, organics collected on 29 September. (c) Mixing of SIA and fly ash, soot, organics collected on 10 October. Organics are heterogeneously mixed with SIA.

Table 1 Concentrations of six air pollutants during the sampling period, two pollution periods, and clean period

Pollutants	All data		polluted period-1		polluted period-2		other period	
	mean ±SD Max, Min	n	mean ±SD Max, Min	n	mean ±SD Max, Min	n	mean ±SD Max, Min	n
$PM_{2.5}$	17.06 ±11.39 68.70, 0.20	715	17.6 ±11.46 59.10, 0.20	152	24.45 ±15.12 68.70, 0.30	99	15.32 ±10.41 62.80, 0.20	464
BC	0.54 ±0.42 3.73, 0.02	805	0.55 ±0.52 3.73, 0.04	176	0.85 ±0.50 2.04, 0.02	119	0.47 ±0.40 3.73, 0.03	510
SO_2	1.27 ±1.34 13.93, 0.02	8822	1.2 ±0.99 8.43, 0.20	1981	2.73 ±3.09 13.93, 1.41	1063	1.03 ±0.65 8.43, 0.02	5778
NO_X	2.05 ±1.96 9.86, 0.31	8842	2.37 ±1.33 9.33, 0.65	2001	3.41 ±1.70 9.59, 0.55	1063	1.69 ±0.97 9.33, 0.31	5778
CO	44.78 ±48.03 318.00, 0.20	7822	63.45 ±55.59 318.00, 0.20	1939	104.23 ±54.69 272.40, 0.60	1030	24.68 ±39.91 318.00, 0.20	4853
O_3	50 ±7.86 98.63, 20.43	8817	47.87 ±7.70 67.70, 26.66	2000	49.01 ±10.00 98.63, 20.43	1039	50.53 ±7.56 96.77, 26.66	5778

All data period: 10 Sept.-15 Oct. 2013; Polluted period-1: 18 Sept.-25 Sept. 2013; Polluted period-2: 11 Oct.-15 Oct. 2013